MADRID
inter.noise 2019
June 16 - 19
NOISE CONTROL FOR A BETTER ENVIRONMENT

Noise prediction method for serrated blade of wind turbine based on semi-empirical equations

Han, Dongyeon[1]
Choi, Jihoon[2]
Lee, Soogab[3]
Seoul National University
Department of Mechanical and Aerospace Engineering, Seoul National University
Seoul, 151-744, Republic of Korea

ABSTRACT

Reduction of the noise of wind turbine has been studied by various methods such as controlling the wind turbine blade, designing low noise emissive wind turbine blade and trailing edge serrations. Among these, serration is considered as an effective noise reduction method. Various studies have been carried out to understand the effects of the parameters of the serration. However, most studies have the fixed-wing concepts, and there have been few studies to analyse the noise reduction or to develop a prediction method of the rotor-type blades. Therefore, in this paper, a noise prediction method composed of two noise prediction tools for a wind turbine with trailing edge serrations is proposed. From flow information obtained by an In-house program, WINFAS, the noise from non-serrated blades is obtained by an airfoil self-noise prediction method. Thereafter, the degree of noise reduction caused by the trailing edge serrations is predicted by Lyu's method. The amount of the noise reduction is subtracted from the result predicted before as the noise of the non-serrated blade and the total reduction of the noise from the rotor blades is calculated.

Keywords: Wind turbine, Serration, Noise reduction
I-INCE Classification of Subject Number: 38

1. INTRODUCTION

The wind turbine noise has adverse effects on the residents living around the wind turbine and it causes a retardation of an installation of a new wind farm. In order to overcome these problems, there have been lots of research in various methods to reduce the noise emission from wind turbine. Such methods are composed of controlling pitch

[1] gksehddus@snu.ac.kr
[2] cjh1122@snu.ac.kr
[3] solee@snu.ac.kr

of an existing wind turbine, developing low noise emission airfoil, attaching porous materials on the blade surface and trailing edge serrations, etc. The trailing edge serrations have been shown to be more effective in noise reduction compared to other methods. The trailing edge serrations mean that a shape of the trailing edge has periodical chord lengths in the spanwise direction. Especially, sawtooth shape serrations are known as the most effective geometry of the serrations.

The trailing edge serrations are studied in many research. Amiet proposed a semi-analytical model whose target geometry is a flat plate[1]. Using the Schwarzschild's problem, the scattered pressure on the surface of the flat plate could be obtained. From the scattered pressure field, the far-field sound pressure was calculated using a surface pressure integral. However, this method assumed an infinite chord which means the leading edge cannot affect to the flow around the trailing edge. This induces problems in low frequency range of the predicted noise. In order to overcome this weakness, Roger & Moreau proposed a backscattered pressure from the leading edge and they found that the backscattering could be neglected if the Helmholtz number $kc > 1$. Following the first theory of the Amiet, Howe proposed a new theoretical model based on a semi-infinite plated whose trailing edge is serrated as sinusoidal or sawtooth shapes[2, 3]. It was found that the use of the sawtooth trailing edge is more efficient in the noise reduction than the use of the sinusoidal one. Also, the degree of reduction is larger in case of $2h/\lambda > 8$ where $2h$ and λ are the amplitude and wavelength of the serration, respectively. However, the method proposed by Howe has drawbacks in the degree of noise reduction. The magnitude of the noise reduction is more than 20 dB in some cases, which is much larger than experimental data.

Various experimental investigations on the trailing edge serrations have been conducted in the past. Dassen *et al.* performed noise measurements in both cases of the airfoil and flat plate [4]. Various shapes were tested and they found that the noise reduction of maximum 10dB and 8dB can be achieved in the flat plate and the airfoil respectively. Gruber performed an experimental investigation on several sawtooth trailing edge shapes [5]. The maximum of 5 dB in low frequency range was reduced, but the components in higher frequency region are increased about 4-5 dB.

In order to overcome the overprediction of Howe's method, Lyu *et al.* proposed a new theory that considers the constructive effects induced by the trailing edge serrations[6]. This method includes an iterative procedure to obtain the solutions of a coupled wave equation. The results from the method were validated with those from a finite element simulation. While such methods to predict the noise from the trailing edge serrations have been developed, there have been little attention on the application of the methods on the rotor, especially, on the wind turbine. So, the development of the trailing edge serrations should have been performed by experiments.

The main objective of this study is to develop a method to predict the effects of the trailing edge serrations attached to the wind turbine based on the results studied on the fixed wing cases. Overall process is composed of the prediction of aerodynamics, noise of the wind turbine without the serrations and the effects of the trailing edge serrations. The aerodynamics are predicted through an In-house program, named WINFAS [7], based on Vortex Lattice Method(VLM). Using the results from the aerodynamics, the noise pre diction of the wind turbine without the serrations is performed considering the tonal noise and the airfoil self noise[8, 9]. Next, the effects of the rotor blade with the trailing edge serrations are calculated using the method proposed by Lyu *et al.* Both tools to predict the noise components are expanded to the rotor through a strip theory. Finally, the degrees of noise reduction predicted in the process of the serration parts are subtracted from the preceding results.

2. METHODOLOGY

2.1 Overall process

In order to predict the noise from a wind turbine with trailing edge serrations, four programs are used. At the beginning, aerodynamic coefficients and boundary layer thickness values of the airfoils used in each section of the target wind turbine blade are obtained by a program based on SU2 CFD open source. The aerodynamic coefficient tables and the boundary layer thickness tables are transferred to the next programs shown as the figure 1. From the wind turbine flow analysis tool, flow properties of each section of the blade at each time are obtained. Following the rotor aerodynamics analysis tool, two noise prediction tools are executed using the boundary layer thickness tables and the results from the wind turbine flow analysis tool. The noise prediction process is composed of two stages. In the first stage, components of the airfoil self noise are predicted based on the research of Brooks, *et al.* In the second stage, the degree of the noise reduction by the trailing edge serrations is predicted.

2.1 Dynamics : Vortex Lattice Method

Under the assumptions of incompressible, inviscid and irrotational flow, the equation governing the entire flow regions around the wind turbine except the blade boundary and wake regions becomes Laplace equation, Equation 1,

$$\nabla^2 \Phi^* = 0 \tag{1}$$

where Φ^* means a velocity potential. The general solutions of the Laplace equation are obtained as a combination of sources and doublet distributions. However, the terms could be substituted by vortex lattices along the camber surface in the Vortex Lattice Method(VLM). After the substitution, the velocity potential can be expressed as Equation 2, where Γ is a circulation strength and Φ_∞ is a velocity potential of the free stream.

$$\Phi^* = \frac{1}{4\pi} \int_{body+wake} \Gamma \frac{\partial}{\partial n}\left(\frac{1}{r}\right) dS + \Phi_\infty \tag{2}$$

To obtain the circulation strength of each lattice, Neumann boundary condition for velocity component(i.e. normal velocity component at boundary is zero) is applied, such as Equation 3.

$$\nabla\Phi^* \cdot \hat{n} = \left[\frac{1}{4\pi} \int_{body+wake} \Gamma \nabla\left\{\frac{\partial}{\partial n}\left(\frac{1}{r}\right)\right\} dS + \nabla\Phi_\infty\right] \cdot \hat{n} = 0 \tag{3}$$

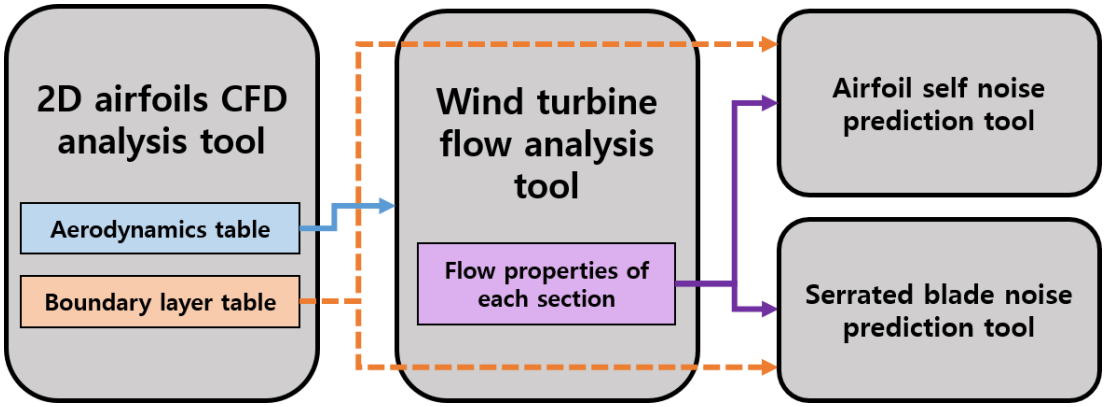

Figure 1. Overall process of the prediction of the wind turbine with trailing edge serrations.

In a rotor case, the freestream velocity(V_0) and the rotational velocity($\vec{\Omega} \times \vec{r}$) should be considered, too. Considering the terms, the discretized form of the governing equation to obtain the circulation strengths is expressed as Equation 4. Each terms in Equation 4 are from Equation 5 to 7.

$$\left[\frac{1}{4\pi}\sum_{body}\Gamma\nabla\left\{\frac{\partial}{\partial n}\left(\frac{1}{r}\right)\right\}+\frac{1}{4\pi}\sum_{wake}\Gamma\nabla\left\{\frac{\partial}{\partial n}\left(\frac{1}{r}\right)\right\}+\left(V_0+V_{pitch}+\Omega\times r\right)\right]\cdot n=0 \tag{4}$$

$$[a_{ij}]\{\Gamma_j\}=\{RHS_j\} \tag{5}$$

$$a_{ij}=\left[\frac{1}{4\pi}\nabla\left\{\frac{\partial}{\partial n_i}\left(\frac{1}{r_{ij}}\right)\right\}\right]\cdot n_i \tag{6}$$

$$RHS_{\mathrm{j}}=-\left[\frac{1}{4\pi}\sum_{wake}\Gamma\nabla\left\{\frac{\partial}{\partial n_i}\left(\frac{1}{r_{ij}}\right)\right\}+\left(V_{0,i}+v_{rel,i}+\Omega_i\times r_{ij}\right)\right]\cdot n_i \tag{7}$$

2.2 Noise : Airfoil self noise

Noise is generated even in the case of a steady state. Vorticities in the boundary layer are able to interact with the surface of the blade and noise can be induced by the interaction. These noises are categorized as the following components based on their generation mechanism. Also, all the components are expanded to the rotor by a concept of a strip theory. Additionally, an observer position is set to reference position 1 of IEC 61400-11[10].

2.2.1 Turbulent Boundary Layer Trailing Edge Noise(TBLTE)

The boundary layer generated from the stagnation point of an airfoil experience a transition to a turbulent flow. The turbulence in the boundary layer cause a perturbing pressure field. This pressure field is generally an inefficient acoustic source which is proportional to the 6th power of the Mach number, M^6, but it could be a strong acoustic source if it interact with sharp edges like the trailing edge of the airfoil. The noise caused by these mechanism is called the turbulent boundary layer trailing edge noise(TBLTE) and it is composed of the noise from the suction side, pressure side and stall with separation like the Equation 8. The Equation 9 and 10 express the noise from the suction and the pressure side, respectively.

$$SPL_{TBLTE}=10\log_{10}(10^{SPL_s/10}+10^{SPL_p/10}+10^{SPL_\alpha/10}) \tag{8}$$

$$SPL_s=10\log_{10}\left(\frac{\delta_s^*M^5D_hL}{r^2}\right)+G_A\left(\frac{St_s}{St_1}\right)+(K_1-3) \tag{9}$$

$$SPL_p=10\log_{10}\left(\frac{\delta_p^*M^5D_hL}{r^2}\right)+G_A\left(\frac{St_p}{St_1}\right)+(K_1-3)+\Delta K_1 \tag{10}$$

2.2.2 Separation and Stall noise(SEP)

As mentioned above, one of the components that are included in the TBLTE noise is a generated by the separation and the stall. It is expressed as the Equation 11.

$$SPL_\alpha=10\log_{10}\left(\frac{\delta_s^*M^5D_hL}{r^2}\right)+G_B\left(\frac{St_s}{St_1}\right)+K_2 \tag{11}$$

2.2.3 Laminar Boundary Layer Vortex Shedding noise(LBLVS)

In case of a low Reynolds number flow, the transition which is aroused on the surface of the airfoil is not triggered. So, the laminar state is kept until the flow arrives at the trailing edge. At this time, the laminar flows become unstable and an unstable state which

is called as Tollmien Schlichtling instability causes the noise in the laminar boundary layer. This noise could be expressed as the Equation 12.

$$SPL_{LBLVS} = 10\log_{10}\left(\frac{\delta_p M^5 D_h L}{r^2}\right) + G_1\left(\frac{St'}{St'_{peak}}\right) + G_2\left(\frac{Re}{Re_0}\right) + G_3(\alpha) \quad (12)$$

2.2.4 Tip noise

Vorticities are generated at the blade tip because of the strong pressure gradient. These vorticities interact with the tip region and it cause the noise which has a similar mechanism with the TBLTE. The following equation, Equation 13, expresses the tip noise.

$$SPL_{TIP} = 10\log_{10}\left(\frac{M^2 M_{tv}^3 D_h l_{tv}^2}{r^2}\right) - 30.5(logSt'' + 0.3)^2 + 126 \quad (13)$$

2.2.5 Blunt Trailing Edge noise(TEBVS)

Generally, the trailing edge could not be manufactured as a sharp shape because of some structural problems, production or installation, etc. This blunt trailing edge shape cause a strong vorticity at the trailing edge region expressed as the Equation 14. This vorticity makes a noise which has a tonal property.

$$SPL_{TEBVS} = 10\log_{10}\left(\frac{t^* M^{5.5} D_h L}{r^2}\right) + G_4\left(\frac{t^*}{\delta^*_{avg}}, \Psi_{TE}\right) + G_5\left(\frac{t^*}{\delta^*_{avg}}, \Psi_{TE}, \frac{St''}{St''_{peak}}\right) \quad (14)$$

2.3 Noise : Trailing edge-serrated blade noise

The airfoils considered in this study are basically assumed as a flat plate airfoil. Figure 2 shows the flat plate airfoil whose chord and span lengths are c and d, respectively. The trailing edge serration is defined by the amplitude h and the wave length λ. The body-fixed coordinate is denoted by x_1, y_1, z_1 as shown in the figure. The observer point is located at (x', y', z'). The wall pressure coming from the leading edge is assumed to have temporal and spatial periodicity by the turbulence and it is expressed as the following form, Equation 15.

$$p_i = P_i e^{-i(\omega t - k_1 x_1 - k_2 x_2)} \quad (15)$$

P_i in the equation is the magnitude of the incident wall pressure gust. The gust has a temporal periodicity, ω, and chordwise and spanwise periodicity, k_1 and k_2, respectively.

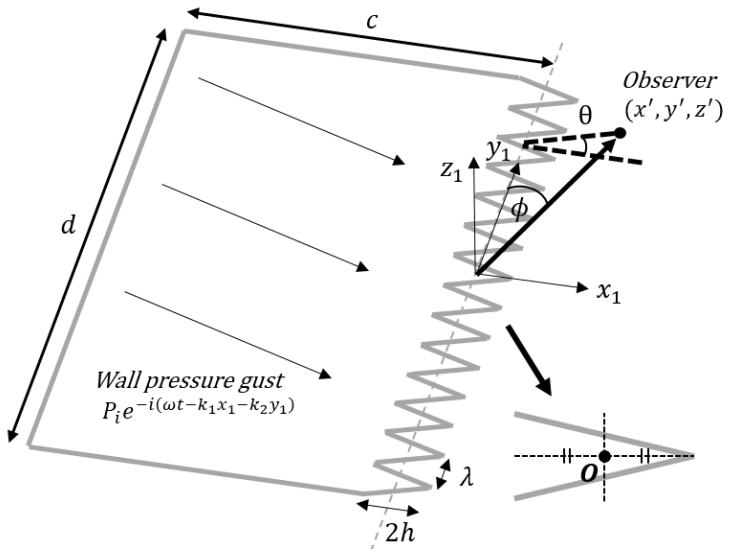

Figure 2. Ideal flat plate with trailing edge serrations, reproduced from [6].

The incident pressure field(p_i) induces a scattered pressure field(p_s) developed from the trailing edges at which the boundary condition is changed abruptly [1]. Although the boundary condition is changed at the trailing edge, the Kutta condition should be satisfied. Thus, the incident pressure is offset by the scattered pressure field. The total pressure(p_t) is composed of the two pressure terms.

The scattered pressure field, p_s, must satisfy the following boundary condition at $z_1 = 0$. In the Equation 16, the function, $x = H(y_1)$, describes the shape of the trailing edge. The function is defined as the Equation 17. Also, the scattered pressure is governed by the wave equation outside the boundary layer in which the flow have a speed of U. The Equation 18 shows the wave equation where c_0 and U represents the speed of sound and the ambient mean flow velocity.

$$\begin{cases} \dfrac{\partial p_s}{\partial z_1} = 0\,, & x_1 < H(y_1) \\ p_s = -P_i e^{-i(\omega t - k_1 x_1 - k_2 x_2)}\,, & x_1 \geq H(y_1) \end{cases} \tag{16}$$

$$H(y_1) = \begin{cases} \sigma_0(y_1 - b_1 - m\lambda) + a_1 \;\;, & b_1 + m\lambda < y_1 \leq b_2 + m\lambda \\ \sigma_1(y_1 - b_2 - m\lambda) + a_2 \;\;, & b_2 + m\lambda < y_1 \leq b_3 + m\lambda \end{cases} \tag{17}$$

$$\nabla^2 p_s - \frac{1}{c_0^2}\left(\frac{\partial}{\partial t} + U\frac{\partial}{\partial x_1}\right)^2 p_s = 0 \tag{18}$$

If the scattered pressure field is assumed to be a harmonic perturbation as the Equation 19, the above wave equation, Equation 18, is modified like the Equation 20 where $\beta = 1 - M_0^2$, $k = \omega/c_0$ and $M_0 = U/c_0$.

$$p_s = P(x_1, y_1, z_1)e^{-i\omega t} \tag{19}$$

$$\beta^2\frac{\partial^2 P}{\partial x_1^2} + \frac{\partial^2 P}{\partial y_1^2} + \frac{\partial^2 P}{\partial z_1^2} + 2ikM_0\frac{\partial P}{\partial x_1} + k^2 P = 0 \tag{20}$$

Roger, Schram and Santana proposed a coordinate transformation to make the boundary condition, Equation 16, independent of y_1 [11]. The new coordinate is defined as the Equation 21 and Equation 22 and 23 are about the modified boundary condition and wave equation, respectively.

$$\begin{cases} x = x_1 - H(y_1) \\ y = y_1 \\ z = z_1 \end{cases} \tag{21}$$

$$\begin{cases} \dfrac{\partial P(x,y,0)}{\partial z} = 0\,, & x < 0 \\ P(x,y,0) = -P_i e^{i(k_1 x + k_2 y)} e^{ik_1 H(y)}\,, & x \geq 0 \end{cases} \tag{22}$$

$$\left(\beta^2 + H'^2(y_1)\right)\frac{\partial^2 P}{\partial x^2} + \frac{\partial^2 P}{\partial y^2} + \frac{\partial^2 P}{\partial z^2} - 2H'(y)\frac{\partial^2 P}{\partial x \partial y} + \left(2iM_0 k - H''(y)\right)\frac{\partial P}{\partial x} + k^2 P = 0 \tag{23}$$

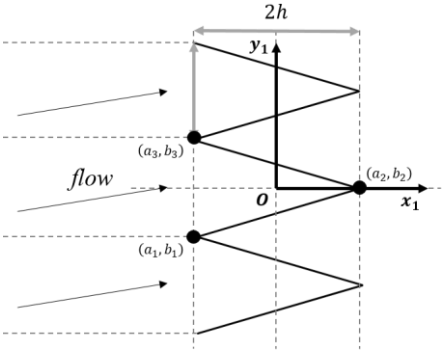

Figure 3. Geometry of the sawtooth serrations, reproduced from [6].

The scattered pressure is assumed to be periodic in the spanwise direction. It could be, then, expanded as a Fourier series in the direction like

$$P(x,y,z) = \sum_{n=-\infty}^{\infty} P_n(x,z)e^{ik_{2n}y} \tag{24}$$

where $k_{2n} = k_2 + 2n\pi/\lambda$. Also, the wave equation, Equation 23, could be modified as

$$\left\{\left(\beta^2 + H'^2(y)\right)\frac{\partial^2}{\partial x^2} + \frac{\partial^2}{\partial y^2} + \frac{\partial^2}{\partial z^2} - 2H'(y)\frac{\partial^2}{\partial x \partial y} + \left(2iM_0k - H''(y)\right)\frac{\partial}{\partial x} + k^2\right\} \times \sum_{n=-\infty}^{\infty} P_n(x,z)e^{ik_{2n}y} = 0 \tag{25}$$

By multiplying Equation 25 by $e^{-ik_{2n'}y}$ and integrating from $-\lambda/2$ to $\lambda/2$, the Equation 25 is modified to the Equation 26.

$$\left\{\beta^2\frac{\partial^2}{\partial x^2} + \frac{\partial^2}{\partial z^2} + 2ikM_0\frac{\partial}{\partial x} + \left(k^2 - k_{2n'}^2\right)\right\}P_{n'}(x,z) + \frac{1}{\lambda}\int_{-\lambda/2}^{\lambda/2}\sum_{n=-\infty}^{\infty}\left\{H'^2(y)\frac{\partial^2}{\partial x^2} - \left(H''(y) + 2ik_{2n}H'(y)\right)\frac{\partial}{\partial x}\right\}P_n(x,z)e^{i\left[\frac{2(n-n')\pi}{\lambda}\right]y}dy = 0 \tag{26}$$

In the above equation, H' and H'' are defined using the conventional generalized function.

$$H'(y_1) = \begin{cases} \sigma_0 = \dfrac{b_2 - b_1}{a_2 - a_1}, & b_1 + m\lambda < y_1 \le b_2 + m\lambda \\ \sigma_1 = \dfrac{b_3 - b_2}{a_3 - a_2}, & b_2 + m\lambda < y_1 \le b_3 + m\lambda \end{cases} \tag{27}$$

$$H''(y_1) = \sum_{m=-\infty}^{\infty}(-1)^{m+1}2\sigma\delta(y_1 - m\lambda/2) \tag{28}$$

Using a formation, $\int_{-\infty}^{\infty} f(x)\delta(x-\tau)dx = f(\tau)$, the wave equation can be modified as

$$\left\{(\beta^2 + \sigma^2)\frac{\partial^2}{\partial x^2} + \frac{\partial^2}{\partial z^2} + 2ikM_0\frac{\partial}{\partial x} + \left(k^2 - k_{2n'}^2\right)\right\}P_{n'}(x,z) = -\frac{4\sigma}{\lambda}\sum_{n-n'=odd}\left(1 - \frac{k_2\lambda + 2n\pi}{(n-n')\pi}\right)\frac{\partial P_n(x,z)}{\partial x} \tag{29}$$

Also, the boundary condition could be modified by the Fourier transform as

$$\begin{cases} \dfrac{\partial P_n(x,0)}{\partial z} = 0, & x < 0 \\ P_n(x,0) = -P_i a_n e^{ik_1 x}, & x \ge 0 \end{cases} \tag{30}$$

The next steps in detail for the numerical method are contained in the Lyu's paper[6]. Following the procedures in the paper, the degrees of the noise reduction by the airfoil with trailing edge serrations can be obtained. In common with the airfoil self noise prediction, this method is applied in each section based on the strip theory.

2.4 Noise : Subtraction

From the methods explained above, two spectrum data for the airfoil self noise and the degree of noise reduction by serrations is obtained. In order to predict the noise of rotor

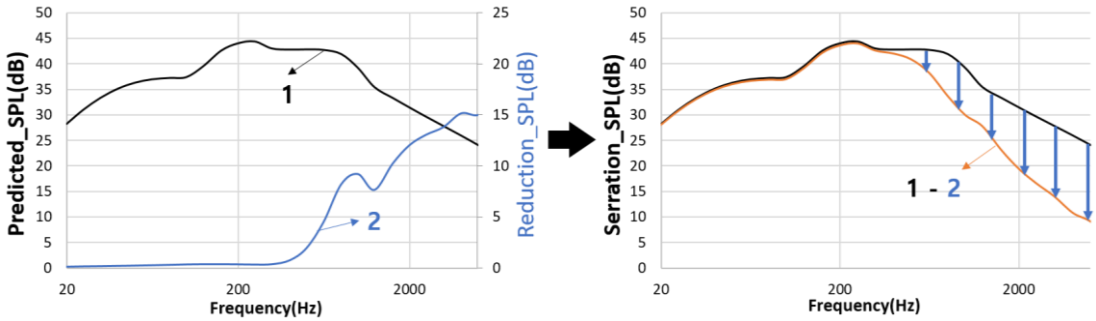

Figure 4. Spectrum subtraction by two predicted spectrum

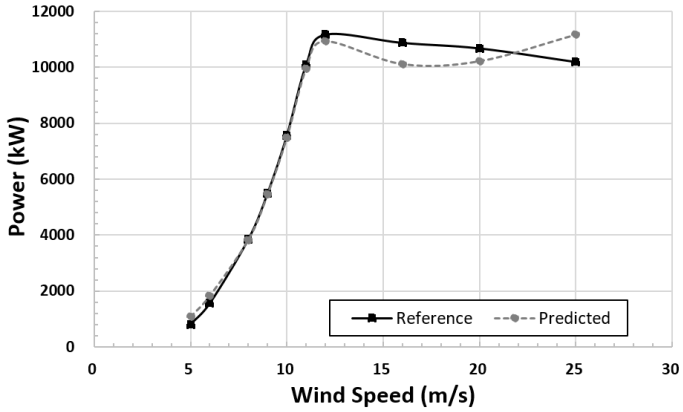

Figure 5. Power curves of the RWT reference and results of In-house program(WINFAS).

with trailing edge serrations, the degree of reduction by serration is subtracted from the predicted noise of the rotor blade without serrations like figure 4. Following this process, the predicted noise of the noise from the trailing edge serrated rotor blades.

3. RESULTS AND DISCUSSION

Validations of the In-house program for the wind turbine aerodynamics, WINFAS, and the noise prediction are performed on the DTU 10MW Reference Wind Turbine and NREL AOC 15/50 50KW wind turbine[12, 13]. Also, the degree of the noise reduction of the trailing edge serrations of a flat plate, not rotor case, is validated by comparing the prediction results with the results of the Lyu's paper [6].

3.1. Validation of wind turbine aerodynamics

The aerodynamics of the wind turbine are validated with the DTU 10MW Reference Wind Turbine[12]. As shown in the figure 5, the aerodynamic power generated by the wind turbine is very similar under the wind speed condition that the wind turbine is regulated. Although the power curves are not matched each other over the conditions, the errors are under 5% of the power generated in each wind speed. The In-house program, WINFAS, is said to be well validated, especially under the rated power condition.

3.2. Validation of wind turbine noise

The predicted noise in frequency domain is compared with the AOC 15/50 wind turbine experimental data [13]. Only the dominant components of the airfoil self noise are presented in the figure 6. As shown in the figure, components in frequency region of 100 ~ 1000 Hz follow the tendency of the experimental data. However, the other regions, low and high frequency range, are not matched with the experimental data well. The low frequency region includes background noise which is not considered in the prediction. Also, it seems that the harmonic components of the TEBVS exist in the high frequency

range, but they were not considered in this study. Thus, there are some errors in the low and high frequency range because of the two reasons.

3.3. Validation of noise from flat plate with trailing edge serrations

The degree of noise reduction by the trailing edge serrations is not quite matched with the experimental data even in the latest research[14]. So, the validation is performed with the data from the Lyu's paper[6]. In the method, there are two parts to increase the accuracy of the prediction. The first one is an integration from $-\lambda/2$ to $\lambda/2$ and the second one is how many higher orders, m, are considered. If the two parts are composed of large values, the accuracy is saturated and the results are same with the results from the Lyu's paper. Therefore, some different cases which result in different accuracy are selected.

In order to integrate some variables in the Lyu's method, the integration method is performed by a Gauss quadrature method. As shown in the figure 7, the larger the number of integration node is, the better the accuracy is, especially in the high frequency region. In this example, the number of nodes of 90 is enough to estimate the frequency region under $kc = 100$. The range of accuracy increase linearly while the number of nodes increases linearly. Thus, it is easy to obtain how many nodes should be used to get accurate values of a target frequency.

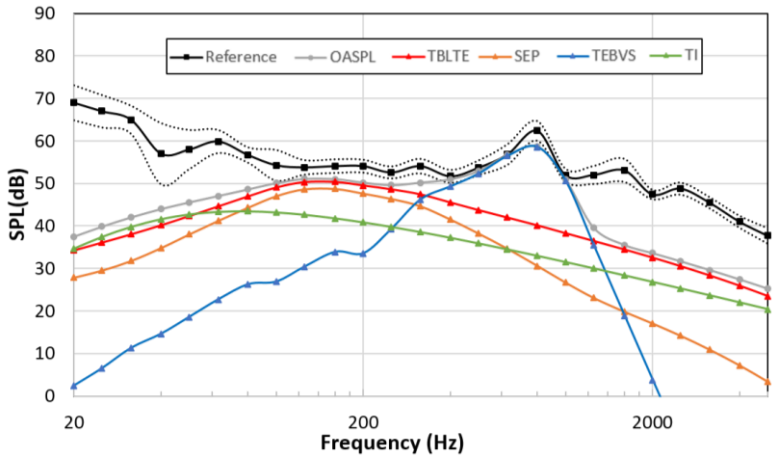

Figure 6. Noise prediction of rotor blade without serrations ,inflow speed of 6m/s, AOC 15/50.

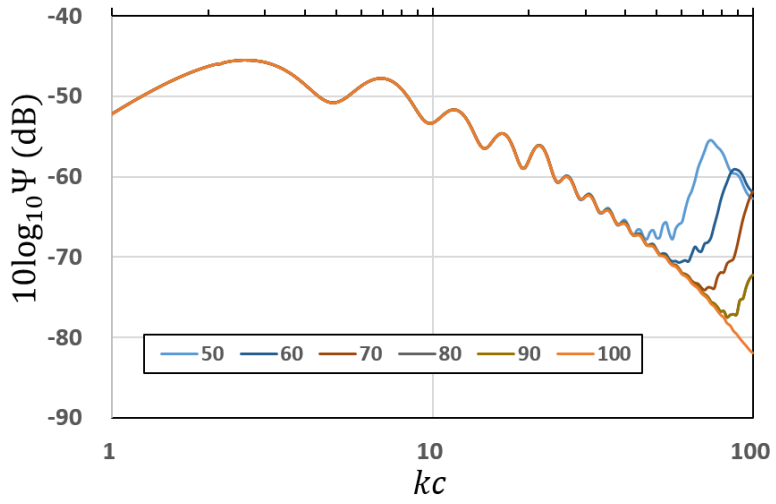

Figure 7. Cases for accuracy test about the number of integration nodes, Ψ is a non-dimensioinalized far-field power spectral density, kc is the number of inident turbulence periods in one chord length.

As shown in the figure 8, the number of higher order terms affects errors in the predicted spectrum. Although the large number of the higher order terms conserves the accuracy in high frequency region, it induces larger computational costs. So, it is important to set a limit considering a trade-off. In this validation case, the number of 10 terms seems to be enough under $kc = 100$. However, more terms are required if the chord length is large because the criterion of the accuracy is kc, the number of incident turbulence periods in one chord length. So, the costs are much higher in case of large wind turbine to apply the method.

For comparison with the results of Lyu's study[6], a prediction result is validated for the case in the study of Lyu *et al*. Figure 9 shows one of the cases that the study handled. The reference data of the figure 9 is extracted and reproduced from the paper. The two curves have similar tendency but the positions and the magnitude of the peaks are slightly different. It seems that the errors are induced by differences of variables inserted in the program like the number of higher order terms considered, etc. Although the two curves are not perfectly matched, the errors are reasonable.

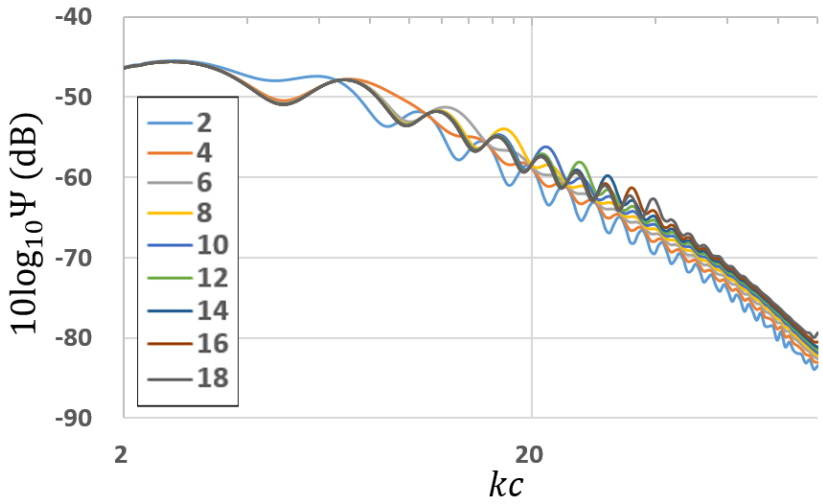

Figure 8. Cases for accuracy test about the number of higher order terms.

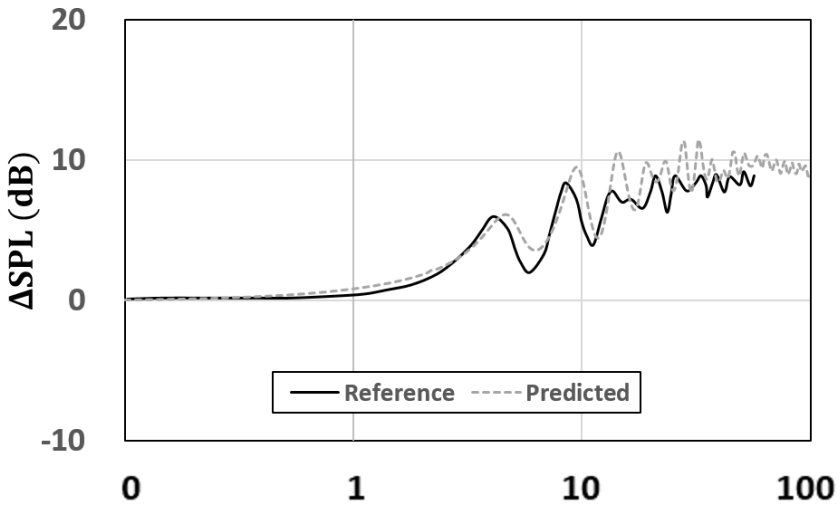

Figure 9. The spectrum of the sound reduction spectrum ΔSPL for an observer at $x_3/c = 1$ and $\theta = 90°$, $\lambda/h = 0.2, h/c = 0.05$.

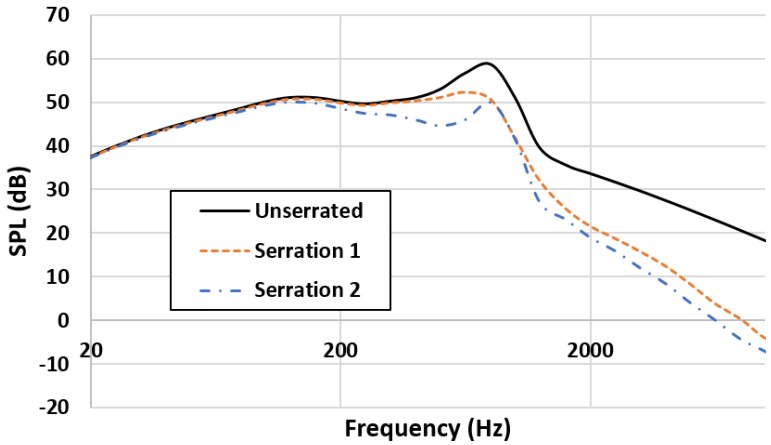

Figure 10. Noise of wind turbine with trailing edge serrations. Serration 1 : h is 0.02 m, λ is 0.002 m, Serration 2 : h is 0.03m, λ is 0.002m

3.4. Trailing edge-serrated wind turbine noise

Following the methods proposed in section 2.4, a trailing edge serrated wind turbine is tested for two trailing edge serrations. In the figure 10, Serration 2 has more sharp serration shape than that of the Serration 1. As already known, the large value of h/λ induces more reduction of the noise. In other words, the Serration 2 whose h/λ is 15 has an advantage over Serration 1, $h/\lambda = 10$. Although the predicted results are not validated with experimental results, the sharp trailing edge reduces noise significantly in the frequency around 1000 Hz. In the high frequency region, it is known that the trailing edge serrations make the noise slightly bigger than the unserrated one[15], but the predicted results show reductions more than 10 dB. So, the high frequency region seems unreliable.

4. CONCLUSIONS

The method proposed by Lyu *et al.* has an advantage in taking not only the destructive effects but also the constructive effects of the trailing edge serrations into account. Therefore, the degree of noise reduction becomes relatively more reasonable than the results of Howe's study. Based on the Lyu's method, an application of the noise prediction method to a wind turbine is performed in this study. The numerical analysis of the aerodynamics of the wind turbine is performed using In-house program, WINFAS, which is based on the VLM. Using the detail flow information such as an effective velocity, angle of attack around the wind turbine rotor obtained by the WINFAS, the noise of the AOC 15/50 wind turbine rotor without serrations is predicted based on the airfoil self noise by the strip theory. These results are validated with the AOC 15/50 experimental results. The predicted noise of the serrated airfoil, not rotor, has similar tendency with the study of Lyu, and the method is applied to the wind turbine based on the strip theory. The results of the trailing edge-serrated wind turbine show that the sharp serration has better effects on the reduction of noise, although the reduction of high frequency region is unreliable because of the difference with the experimental data.

This study suggests a new method to apply the noise prediction method of trailing edge serration to a rotor. Although it has a limit that the Mach number of the flow around the blade should be small, $M \sim 0.2$, it could be applied on the drones or the wind turbines easily. The methodology proposed in this study could be applied on the optimization of the trailing edge serrated rotor if more precise validations is preceded. Therefore, the limits of this study, shortage of validation cases and errors in high frequency region, must be overcome. Future work should therefore include the construction of the experimental data about the trailing edge serrations on a wind turbine and more reliable validations.

5. ACKNOWLEDGEMENTS

This work was supported by the New & Renewable Energy of the Korea Institute of Energy Technology Evaluation and Planning(KETEP) grant funded by the Korea government Ministry of Knowledge Economy (No. 20183010025280) and by Korea Institute of Energy Technology Evaluation and Planning(KETEP) grant funded by the Korea government(MOTIE), (20183010025120, Development of 8MW High Capacity Offshore Wind Turbine).

6. REFERENCES

1. Amiet RK. "*Noise due to turbulent flow past a trailing edge*". Journal of Sound and Vibration. (1976);47(3):387-93.
2. Howe MS. "*Aerodynamic noise of a serrated trailing edge*". Journal of Fluids and Structures. (1991);5(1):33-45.
3. Howe MS. "*Noise produced by a sawtooth trailing edge*". The Journal of the Acoustical Society of America. (1991);90(1):482-7.
4. Dassen T, Parchen R, Bruggeman J, Hagg F. "*Results of a wind tunnel study on the reduction of airfoil self-noise by the application of serrated blade trailing edges*". (1996).
5. Gruber M. "*Airfoil noise reduction by edge treatments*", University of Southampton, (2012).
6. Lyu B, Azarpeyvand M, Sinayoko S. "*Prediction of noise from serrated trailing edges*". Journal of Fluid Mechanics. (2016);793:556-88.
7. Son E, Kim H, Kim H, Choi W, Lee S. "*Integrated numerical method for the prediction of wind turbine noise and the long range propagation*". Current Applied Physics. (2010);10(2):S316-S9.
8. Brooks TF, Pope DS, Marcolini MA. "*Airfoil self-noise and prediction*". (1989).
9. Farassat F. "*Derivation of Formulations 1 and 1A of Farassat*". (2007).
10. Commission IE. "*IEC 61400-11 Wind Turbine Generator Systems—Part 11: Acoustic Noise Measurement Techniques*". Geneva, Switzerland: International Electrotechnical Commission. (2012).
11. Roger M, Schram C, De Santana L, "*Reduction of airfoil turbulence-impingement noise by means of leading-edge serrations and/or porous material*", editor^editors. 19th AIAA/CEAS aeroacoustics conference, (2013).
12. Bak C, Zahle F, Bitsche R, Kim T, Yde A, Henriksen LC, et al. "*Description of the DTU 10 MW reference wind turbine*". DTU Wind Energy Report-I-0092. (2013);5.
13. Huskey A, Link H, Butterfield C. "*Wind turbine generator system acoustic noise test report for the AOC 15/50 wind turbine*". Colorado: Golden. (1999):87.
14. Mayer Y, Lyu B, Kamliya Jawahar H, Azarpeyvand M, "*Toward a Semi-Empirical Noise Prediction for Airfoils with Serrated Trailing Edges*", editor^editors. 2018 AIAA/CEAS Aeroacoustics Conference, (2018).
15. Gruber M, Joseph P, Chong TP, "*Experimental investigation of airfoil self noise and turbulent wake reduction by the use of trailing edge serrations*", editor^editors. 16th AIAA/CEAS aeroacoustics conference, (2010).